Printable and High Performance MnO_2-based Energy Storage Devices

Jiasheng Qian and Shu Ping Lau

The Hong Kong Polytechnic University, Department of Applied Physics,
Hong Kong SAR, apsplau@polyu.edu.hk

ABSTRACT

We report a printable and high performance energy storage device comprising MnO_2-based electrodes and ionogel electrolyte. The MnO_2 based electrodes could be prepared on various substrates by inkjet printing process without any binder. As a result, continuous and semi-transparent MnO_2 thin films were obtained on the commercially available fluorine doped tin oxide (FTO) glass and served as the electrode for symmetric supercapacitor. The as-prepared device exhibited a maximum specific capacitance of 86 $F{\cdot}g^{-1}$ at 0.1 $A{\cdot}g^{-1}$, leading to a superior energy density of 38.75 $Wh{\cdot}kg^{-1}$. All the merits make the MnO_2 based energy storage devices a promising candidate for large-scale production of printable and high performance electronics in the near future.

Keywords: printable electronics, energy storage devices, supercapacitor, inkjet printing, MnO_2 nanosheets

1 INTRODUCTION

The energy storage devices have been paid much attention due to its potential applications ranging from mobile devices, backup power sources, electrical vehicles and wearable/implantable electronics. [1-4] In never-ceasing pursuit of long term usage of these electronic devices, the high performance capacitive energy storage devices, also called supercapacitors, are extremely required. To date, a great deal of efforts has been made. Some representative achievements including supercapacitors with high specific capacitance up to ~2500 $F{\cdot}g^{-1}$, high voltage up to 3.5V and long term stability for 100,000 cycles have all been achieved. [5-7] However, most of these high performance devices are based on a high cost, time-consuming and complicated process with the use of aqueous or organic solution that gives rise to a serious safety concern because a strict packaging process and a separator are required to prevent possible leakage and short circuit between the electrodes. [8, 9] Recently, many of the researches have also focused on this issue. New progresses such as all solid state supercapacitor has been achieved by using polyvinyl alcohol (PVA) based gel electrolyte. [10-12] these devices could reach a voltage of up to 1.8V, nevertheless, at the expense of a complicated process and unsatisfied performance. Hence, a mass production of reliable supercapacitor with high density and high voltage is still lacking.

By virtue of abundance, high theoretical energy capacity, non-toxicity and environmental compatibility, manganese dioxide (MnO_2) is usually regarded as an ideal candidate for the electrode materials of the energy storage devices, especially supercapacitors. As a member of the transition metal oxides (TMOs) family, MnO_2 is well known as an ideal pseudo-capacitance contributor, leading to a high energy density. Unfortunately, MnO_2 also suffers from the poor electrical conductivity and volume expansion during the charge/discharge, resulting in a poor rate capability and cyclic performance. By now, the MnO_2 electrodes could be prepared by various approaches, such as wet chemical processes, direct electrodeposition or chemical deposition on various substrates (e.g. glass, quartz, copper or aluminum foil) [13-16]. These existing preparation methods could still be too complicated and caused superfluous contaminations. Besides, the as-prepared MnO_2 electrodes by these existing preparation methods primarily work with gel electrolyte. [17, 18] A mass production of optimal MnO_2 based supercapacitor with high voltage and high density is still highly sought, which, however, remains a significant challenge.

2 EXPERIMENT

2.1 Electrode and Capacitor Construction

For the preparation of the MnO_2-based electrode, commercially available indium tin oxide/polyethylene terephthalate (ITO/PET) sheet and FTO glass were washed by deionized (DI) water and ethanol for several times, then pre-treated in nitrogen plasma for 5 min. The MnO_2 nanosheets (MnNSs) suspension was prepared according to the previous reports. [19, 20] Consequently, the MnNSs suspension was printed on the FTO glass by an inkjet printing system (Pixdro, LP 50) at 40°C to form a continuous thin film.

For the fabrication of symmetric supercapacitor (SSC), two identical MnO_2 electrodes were assembled for the symmetric supercapacitor configuration. 85wt % 1-butyl-3-methylimidazolium hexafluorophosphate ($BMIm{\cdot}PF_6$) was mixed with 15wt% fumed silica nanopowder under stirring for 5 h to form the ionogel. The $BMIm{\cdot}PF_6$ ionogel was used as the electrolyte. Two MnO_2 electrodes with same weights of active materials were immersed into ionogel for 5 min. Then the device was clamped tightly (to decrease the contact resistance between electrodes) to narrow the space between two electrodes and dried in an oven at 40 °C for 12 h.

TechConnect Briefs 2017, TechConnect.org, ISBN 978-0-9975117-9-6

2.2 Characterization Instruments.

The morphology of MnO_2 electrode was recorded by using scanning electron microscope (SEM) (Hitachi S-4800) and atomic force microscope (AFM, Digital Instrumental Nanoscope IV) in tapping mode.

2.3 Electrochemical Measurements.

All the electrochemical experiments were performed at ambient temperature. All the cyclic voltammograms (CV) and galvanostatic charge-discharge (GCD) measurements were carried out on a CHI 660C electrochemical workstation (CH Instruments). The specific capacitance (C_{sp}, $F \cdot g^{-1}$) was calculated according to the following equations (1):

$$C_{sp} = \frac{\Delta Q}{2 \times \Delta V \times S \times r} \quad (1)$$

where ΔQ is the integrated area of the CV curve; ΔV is the whole range of voltage window; S is the total area or mass of active material on the electrodes; r is the scan rate of CV measurement.

The GCD measurements at various current densities were performed. The specific capacitance (C_{sp}, $F \cdot g^{-1}$) of the electrode was calculated according to the equations (2):

$$C_{sp} = \frac{I \times \Delta t}{\Delta V \times S} \quad (2)$$

where I is the discharge current; Δt is the discharge time; ΔV is the voltage difference within the discharge time Δt; S is the total area or mass of active material on the electrodes.

The gravimetric energy density (E, $Wh \cdot kg^{-1}$) and gravimetric power density (P, $W \cdot kg^{-1}$) were calculated according to the equations (3, 4):

$$E = \frac{1}{2} C_{sp} V^2 \quad (3)$$

$$P = \frac{E}{\Delta t} \quad (4)$$

where C_{sp} is the specific gravimetric capacitance of the capacitor; V is the operating voltage window; Δt is the discharging time.

3 RESULTS AND DISCUSSIONS

Herein we report a high performance MnO_2 based supercapacitor fabricated by a simple inkjet printing process. The MnNSs suspension was firstly prepared *via* a facile approach, followed by printed onto ITO/PET sheet or

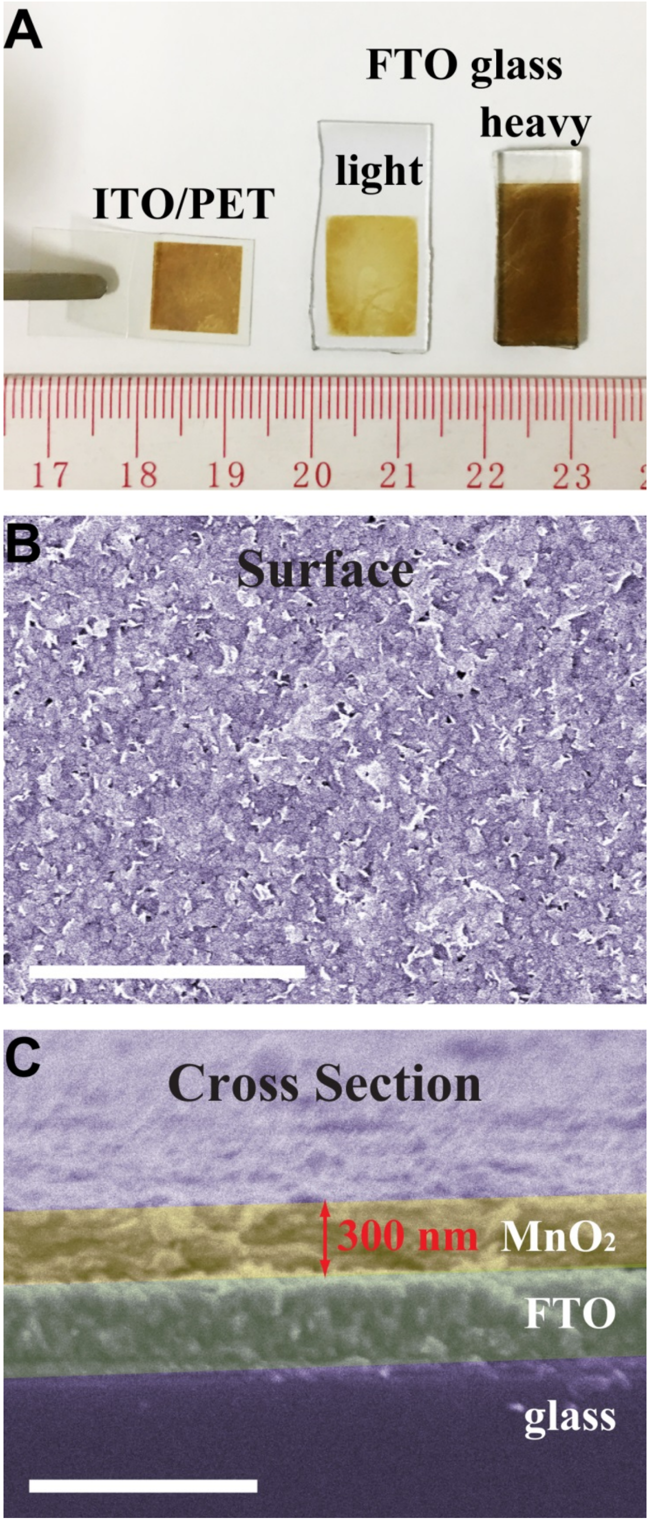

Figure 1. Morphology of the MnO_2 electrode. A) optical image of the MnO_2 electrode on various substrates. B, C) Surface and cross-sectional SEM images of MnO_2 electrode on FTO glass. Scale bars are both 1 μm.

FTO glass with different mass loading to prepare a flexible or semi-transparent electrode, as shown in Figure 1A. The

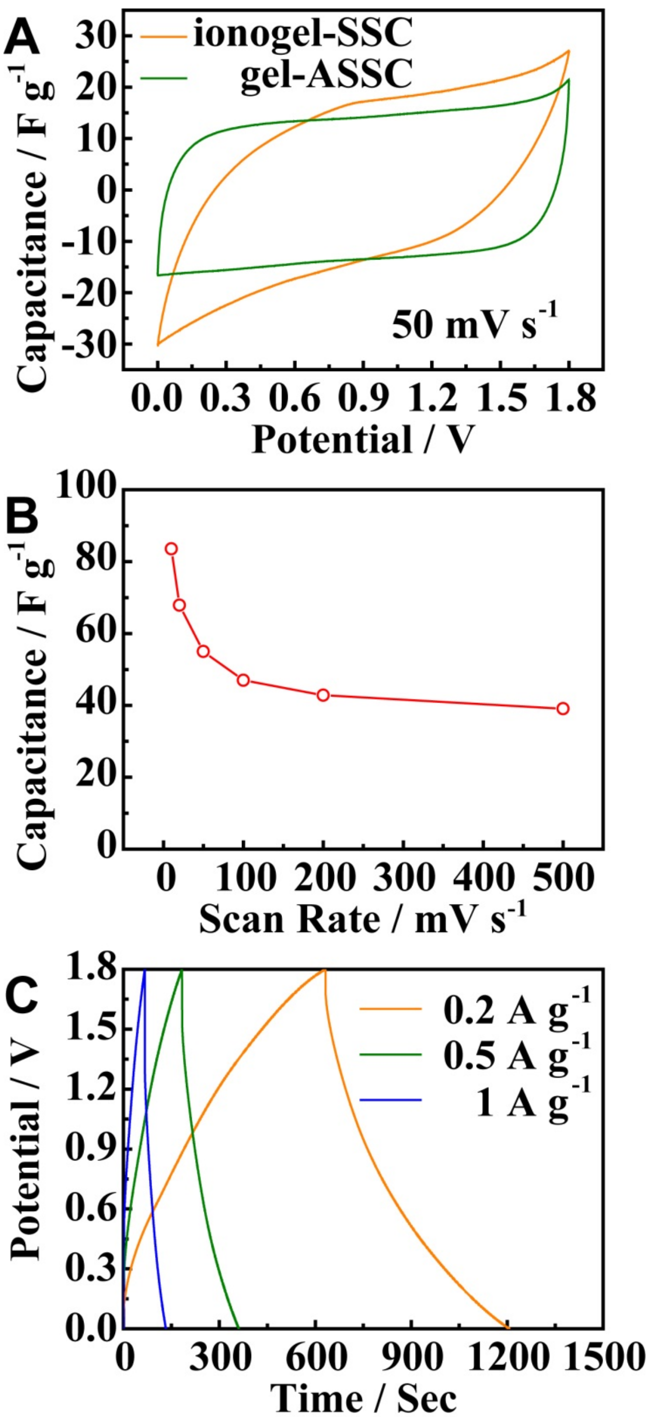

Figure 2. Electrochemical Performance of the ionogel-SSC. A) CV curves of ionogel-SSC and gel-ASSC at 50 mV·s^{-1}. B) Specific capacitance (C_{sp}) versus scan rate at 10-500 mV·s^{-1}. C) GCD curves at 0.2, 0.5 and 1 A·g^{-1} respectively.

transparency could be controlled by the mass loading of MnO_2. For a better understanding of the electrode morphology, the surface and cross sectional SEM images of the MnO_2 electrode were shown in Figure 1B and C. The surface view of the SEM image shows a continuous and homogeneous formation of porous MnO_2 thin film with no obvious cracking or exfoliation. The thickness of the MnO_2 thin film could be ~300 nm which is calculated from the cross sectional SEM image, as shown in Figure 1C. A smooth surface could also be observed, which agrees with the result of surface SEM image in Figure 1B. As reported by previous literature, such a porous and smooth thin film could be ideal for the electrode materials of capacitive energy storage devices. [21]

To investigate the electrochemical properties, the as-prepared MnO_2 electrodes were assembled in a sandwich structure with ionogel electrolyte in between to fabricate a symmetric supercapacitor (denoted as ionogel-SSC). No binder was used during all tests. As shown in Figure 2A, CV curve of the ionogel-SSC exhibits a rectangular-like shape at 50 mV·s^{-1}. Benefiting from the use of organic electrolyte, the voltage of ionogel-SSC could reach 1.8V, which is on the same level of the conventional asymmetric supercapacitors in aqueous or gel electrolyte. [22, 23] Furthermore, a specific capacitance of 55 F·g^{-1} was achieved, which could be even higher than the value of high performance MnO_2 asymmetric supercapacitor (53 F·g^{-1}) in LiCl/PVA gel electrolyte (denoted as gel-ASSC) according to the previous report. [19] As expected, the high energy capacity could be attributed to the porous and homogeneous structure of the MnO_2 thin film, resulting in a high speed ion-transport on electrode/electrolyte interface with rapid charging and discharging characteristics. [24] The specific capacitance of ionogel-SSC versus scan rate curve is shown in Figure 2B. A maximum specific capacitance of 83.6 F·g^{-1} was achieved at 10 mV·s^{-1}, which could be comparable or higher than many current state-of-the-art solid state supercapacitors. [3, 25, 26] Even at a high scan rate of 500 mV·s^{-1}, the specific capacitance of ionogel-SSC could still remain at 39 F·g^{-1}, indicating a superior rate capability. Figure 2C shows the GCD curves of the ionogel-SSC at 0.2, 0.5 and 1 A·g^{-1}, respectively. All curves exhibit triangular shapes, again demonstrating an ideal electrical double layer behavior. A specific capacitance of 73 F·g^{-1} could be reached at 0.2 A·g^{-1}, while 56 F·g^{-1} could be remained when the current density is increased to 1 A·g^{-1}, also showing a desirable rate capability.

For a comprehensive comparison of energy and power densities, the Ragone plots of ionogel-SSC and commercial supercapacitors (SCs) are shown in Figure 3. Notably, the specific energy density of 38.75 Wh·kg^{-1} and the power density of 3.5 kW·kg^{-1} for the ionogel-SSC are much higher than those reported values of commercial SCs. [27, 28] The performance of the ionogel-SSC can be attributed to the homogeneous structure of MnO2 layer and a desirable size match-up between the pores and electrolyte ions.

4 CONCLUSIONS

In summary, a MnO_2 based supercapacitor with high density and high voltage was fabricated by a simple and high efficient inkjet printing system. The as-prepared MnO_2

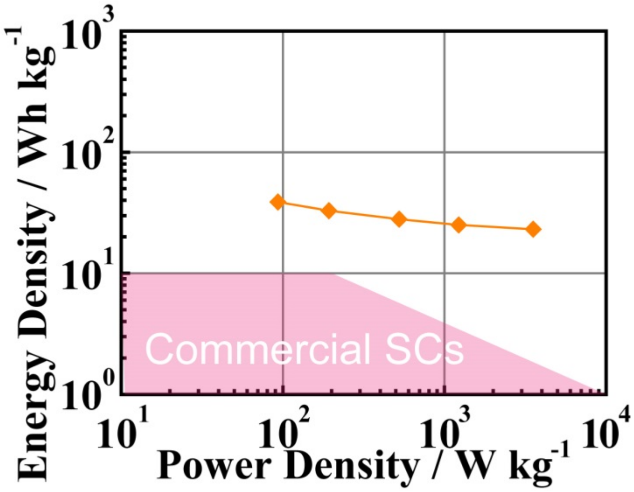

Figure 3. Energy and power densities (Ragone plots) of the ionogel-SSC and commercial supercapacitors (SCs).

electrode exhibits a homogeneous and porous surface morphology with ~300 nm in thickness. The MnO_2 SSC was assembled by using two MnO_2 electrodes with ionogel electrolyte in between. The as-prepared device achieves a high specific energy and power densities as compared to the values of commercial ones. The MnO_2 ionogel-SSC could be a promising candidate as the future energy storage devices. Our findings open up new opportunities for the scalable production of high density and high voltage pseudo-capacitors.

REFERENCES

[1] P. Simon and Y. Gogotsi, Nat. Mater. 7, 845, 2008.

[2] L. Zhang, R. Zhou and X. S. Zhao, J. Mater. Chem. 20, 5983, 2010.

[3] D. Yu, K. Goh, H. Wang, L. Wei, W. Jiang, Q. Zhang, L. Dai and Y. Chen, Nat. Nanotechnol. 9, 555, 2014.

[4] D.-W. Wang, F. Li, M. Liu, G. Q. Lu and H.-M. Cheng, Angew. Chem. Int. Ed. 47, 373, 2008.

[5] M.-K. Song, S. Cheng, H. Chen, W. Qin, K.-W. Nam, S. Xu, X.-Q. Yang, A. Bongiorno, J. Lee, J. Bai, T. A. Tyson, J. Cho and M. Liu, Nano Lett. 12, 3483, 2012.

[6] M. Acerce, D. Voiry and M. Chhowalla, Nat. Nanotechnol. 10, 313, 2015.

[7] Z.-S. Wu, K. Parvez, A. Winter, H. Vieker, X. Liu, S. Han, A. Turchanin, X. Feng and K. Müllen, Adv. Mater. 26, 4552, 2014.

[8] G. Zhou, F. Li and H.-M. Cheng, Energy Environ. Sci. 7, 1307, 2014.

[9] X. Wang, X. Lu, B. Liu, D. Chen, Y. Tong and G. Sehn, Adv. Mater. 26, 4763, 2014.

[10] H. Jin, L. Zhou, C. L. Mak, H. Huang, W. M. Tang and H. L. W. Chan, Nano Energy 11, 662, 2015.

[11] L. Yuan, B. Yao, B. Hu, K. Huo, W. Chen and J. Zhou, Energy Environ. Sci. 6, 470, 2013.

[12] L. Yuan, X.-H. Lu, X. Xiao, T. Zhai, J. Dai, F. Zhang, B. Hu, X. Wang, L. Gong, J. Chen, C. Hu, Y. Tong, J. Zhou and Z. L. Wang, ACS Nano 6, 656, 2012.

[13] Z. Fan, J. Yan, T. Wei, L. Zhi, G. Ning, T. Li and F. Wei, Adv. Funct. Mater. 21, 2366, 2011.

[14] X. Zhao, L. Zhang, S. Murali, M. D. Stoller, Q. Zhang, Y. Zhu and R. S. Ruoff, ACS Nano 6, 5404, 2012.

[15] X. Lu, M. Yu, G. Wang, T. Zhai, S. Xie, Y. Ling, Y. Tong and Y. Li, Adv. Mater. 25, 267, 2013.

[16] G. Yu, L. Hu, N. Liu, H. Wang, M. Vosgueritchian, Y. Yang, Y. Cui and Z. Bao, Nano Lett. 11, 4438, 2011.

[17] P. Yang, Y. Ding, Z. Lin, Z. Chen, Y. Li, P. Qiang, M. Ebrahimi, W. Mai, C. P. Wong and Z. L. Wang, Nano Lett. 14, 731, 2014.

[18] Z. Zhang, F. Xiao, L. Qian, J. Xiao, S. Wang and Y. Liu, Adv. Energy Mater. 4, 1400064, 2014.

[19] J. Qian, H. Jin, B. Chen, M. Lin, W. Lu, W. M. Tang, W. Xiong, L. W. H. Chan, S. P. Lau and J. Yuan, Angew. Chem. Int. Ed. 54, 6800, 2015.

[20] H. Jin, J. Qian, L. Zhou, J. Yuan, H. Huang, Y. Wang, W. M. Tang and H. L. W. Chan, ACS Appl. Mater. Interfaces 8, 9088, 2016.

[21] [12] X. Yang, C. Cheng, Y. Wang, L. Qiu and D. Li, Science 341, 534, 2013.

[22] Z. Su, C. Yang, B. Xie, Z. Lin, Z. Zhang, J. Liu, B. Li, F. Kang and C. P. Wong, Energy Environ. Sci. 7, 2652, 2014.

[23] H. Jin, L. Zhou, C. L. Mak, H. Huang, W. M. Tang and H. L. W. Chan, J. Mater. Chem. A 3, 15633, 2015.

[24] J. Qian, M. Liu, L. Gan, P. K. Tripathi, D. Zhu, Z. Xu, Z. Hao, L. Chen and D. S. Wright, Chem. Commun. 49, 3043, 2013.

[25] G. Sun, X. Zhang, R. Lin, J. Yang, H. Zhang and P. Chen, Angew. Chem. Int. Ed. 54, 4651, 2015.

[26] L. Kou, T. Huang, B. Zheng, Y. Han, X. Zhao, K. Gopalsamy, H. Sun and C. Gao, Nat. Commun. 5, 3754, 2014.

[27] A. Burke, Electrochim. Acta 53, 1083, 2007.

[28] P. Simon and Y. Gogotsi, Acc. Chem. Res. 46, 1094, 2013.